A Control Law for Energy Efficient and Human Like Walking Biped Robot SHERPA Based on a Control and a Ballistic Phase - Application on the Cart-Table Model

Marc Bachelier, Sébastien Krut, Ahmed Chemori

A Control Law for Energy Efficient and Human Like Walking Biped Robot SHERPA Based on a Control and a Ballistic Phase - Application on the Cart-Table Model

Marc BACHELIER, Ahmed CHEMORI, Sébastien KRUT

LIRMM, France, marc.bachelier@lirmm.fr, ahmed.chemori@lirmm.fr, sebastien.krut@lirmm.fr

Abstract— This work proposes a new control approach for biped walking robots. Its purpose is to make human-like robots walk more smoothly and more efficiently with regard to energy. Thus, it is based on the decomposition of a step into two phases: a control phase which prepare a ballistic phase. As a first step towards more complex studies, the tools are simple and efficient: Lagrangian model, Newton's impact law, non-linear quadratic optimization problems used for trajectory planning and partial feedback linearization used for trajectory tracking. Although the final prototype will be the biped robot SHERPA, this control law has been implemented and tested on a simpler one: the cart-table. Numerous simulation results are presented with two concrete examples.

Index Terms— biped robots walking, impacts, trajectory planning, trajectory planning, optimization, linearization

I. INTRODUCTION

The most critical specificity of biped robots are their dynamic balance during walking or the adaptability of their trajectory to the change in their environment. But some different purposes may be specified.

The most popular control approaches to ensure dynamic balance during walking from now on are based on ZMP (Zero-Moment Point) [1] or on similar indicator related to the dynamic of the robot. Numerous famous works have been done in this way. Among them AIST [2] plans the trajectory of the CoM (Center of Mass) so that the ZMP lies always inside the support polygon. The design of the control law of the robot ASIMO from HONDA [3] is known to use the ZMP. Numerous indicators like FRI (Foot Rotation Indicator) and ZRAM (Zero Rate of change of Angular Momentum) [4] have been created and implemented in order to characterize dynamic balance.

Some other approaches try to achieve radically different goals. For instance the robot Rabbit [5] is an underactuated biped robot with adaptive speed. The robot Runbot [6] uses learning techniques in order to master a wide range of speed. Finally a control law for the robots from the MIT [7] were designed to ensure a strong adaptability to rough terrain, this work leading to the well-know Big Dog robot.

The manufacture of our robot SHERPA is in progress. Its purpose is the transport of a light load in an office-like environment with possible stairs (this issue will be discussed in a future paper). Two stereo omnidirectional cameras on
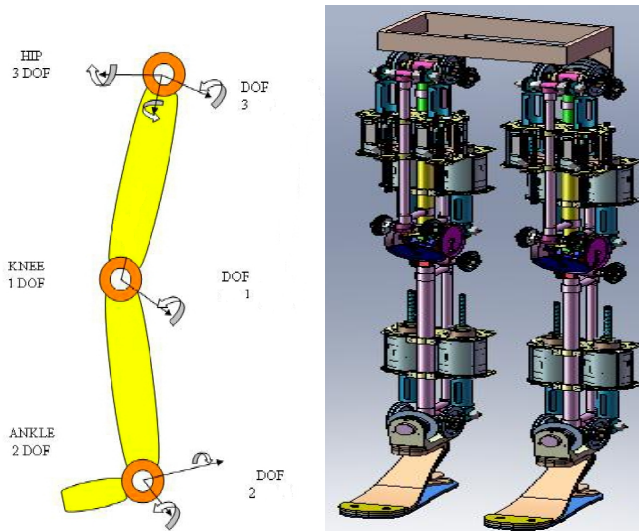

Fig. 1. The mechanical structure of SHERPA with six degrees of freedom on each leg

top of its structure will enable it to follow somebody and to tune its speed to the one of its leader.

SHERPA is a two-legged robot with six degrees of freedom on each leg but no trunk as shown on figure 1. The six degrees of freedom will be totally actuated thanks to linear motor along with cable transmission [8]. The characteristics of this technology is the small inertia and the full reversibility. SHERPA will be 1m tall and will weight 30 kg.

SHERPA has been designed to fit with two specificity. The first one is an energetically effective use of free dynamics. A better use of impacts on the ground and disturbances in the direction of the walking is the final goal. Thus the mechanical design was led with such ideas as complete reversibility of the actuators and compliant feet in mind. Consequently it was obvious that the design of the control law should be oriented towards an optimum use of the energy. The second specificity is a very smooth gait, close to the human one. It implies that we should consider phases of loss and then regain of balance in the direction of walking. Therefore constraining the ZMP inside the support polygon is not interesting in our case.

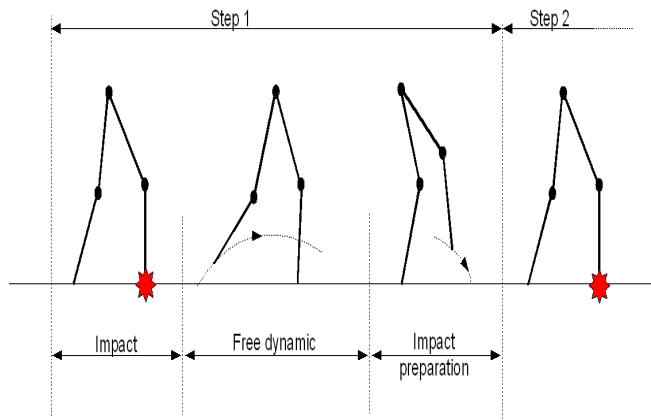Firstly this paper presents the general approach for this

Fig. 2. Decomposition of a step for SHERPA into two phase, the free dynamic and the impact preparation

control law. Then it focuses on its implementation on a simplified model of a biped robot, the cart-table, with details on trajectory planning and tracking. Some results of simulation are shown through two concrete examples. Lastly the numerous opportunities given by this type of control law are listed.

II. AN INNOVATIVE APPROACH FOR SHERPA

A. Presentation of a step of SHERPA

The control of the walking speed of SHERPA must then be based on an energetic aspect. Moreover impact is a critical phase of the walking cycle regarding energy losses. That is why we decided to design the control law around this phase, thus allowing us to get advantage of the compliance of the feet of SHERPA. For any given step length, the choice of an impact speed determines the walking speed of the robot. It becomes then critical to calculate this impact speed and to control it.

A step of SHERPA is shown on figure 2. There is no double support phase: the step is divided into an impact phase and a single support phase, which is itself divided into a free dynamics phase and an impact preparation phase. During the free dynamics phase SHERPA's motion is due to the post-impact energy and the inertia of the robot. While preparing the impact, the foot move so that it will hit the ground with a model-based precalculated speed. This speed involve a precise position and speed of the CoM at the end of the free dynamics phase.

B. A simplified model of SHERPA

A two-dimensional simplified model has been chosen in order to work more rapidly on the control law. It is constituted of a cart moving on top of a table: it is the cart-table. By controlling the force applied on the cart, it is possible to make the table move. The two edges of the foot of the table can be seen as the two feet of the biped robot and the CoM of the cart as its CoM since the mass of the table is considered ten times smaller than the mass of the cart.

mass of the table: M_1	$1kg$
mass of the cart: M_2	$10kg$
total inertia: I_T	$2.5kg.m^2$
height of the cart: h_{G2}	0.5m
height of the table:h_{G1}	0.4m
length of the table foot:P_{max}	0.2m
length of the table top:L_{max}	0.4m

TABLE I

CHARACTERISTICS OF THE CART-TABLE

The cart-table has already been used as a linearized inverse pendulum to model a biped robot during the single support phase [2]. In our study it is used to simulate a complete step with a critical phase, the impact between the table and the ground.

How can we simulate an entire step of a biped robot with such a cart-table? Let's consider a biped robot which walks with a fixed step length. The impact preparation phase seen in figure 2 is obtained with the cart-table when the table swing around its left edge. In this case the cart moves thanks to the motor. Then the instantaneous impact phase on the biped robot (figure 2) occurs with the cart-table when the right edge of the table hit the ground while swinging around the left edge. Finally the free dynamics of the biped robot is obtained with the cart-table when the table swing around its right edge. During this phase the control of the motor is off and the cart can move freely thanks to the reversibility of the motor. A complete step is thus realized. If we want to simulate a second step of the biped robot with the cart-table, it is possible to control the motor while swinging around the right edge and let the cart move freely while swinging around the left edge. So walking of a biped robot correspond to the oscillation of the cart-table moving from left to right or from right to left at each cycle.

In previous work the purpose of the cart-table model was to generate a simplified equation of the dynamics of walking. We have worked further by creating a complete dynamic simulator with matlab and building a mechanical prototype in order to test our control law until SHERPA is available. The simulator is already fully operational and numerous tuning parameters are available (mass, length, friction, initial conditions...). The prototype will be available soon for the first tests. It is constituted of a linear actuator, a force sensor at the foot in order to measure the ZMP and an attitude sensor.

III. DESCRIPTION OF THE CONTROL LAW

A. The Cart-table model

The planar cart-table model shown on figure 3 is an underactuated robot with only one actuator and four degrees of freedom if we consider the full hybrid model (the horizontal and vertical position of the CoM of body 1, x and y, the angle between the ground and the table, θ and the position of the cart on the table, l). Its characteristics are listed in table I.
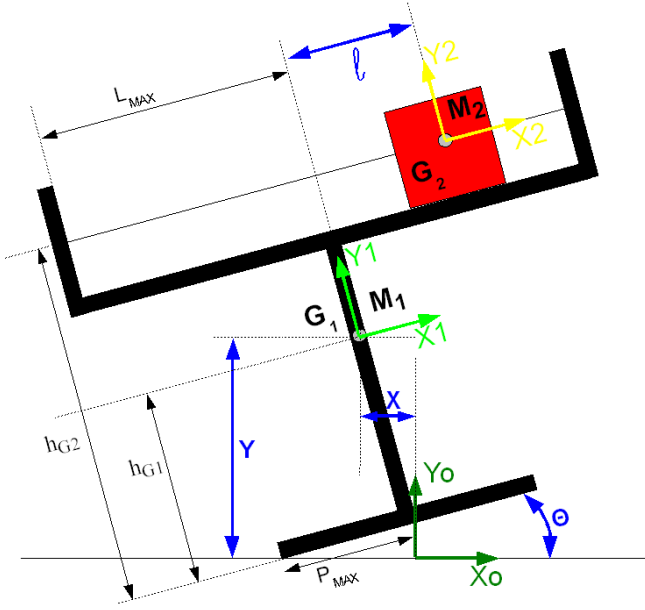
Fig. 3. The cart-table model has four degrees of freedom: $[x, y, \theta, l]$

This model is hybrid because there are different possible contact conditions between the table and the ground: one full contact conditions (equivalent to the double support phase for SHERPA), two symmetric one-point contact conditions (equivalent to the single support phase for SHERPA) and two symmetric impact conditions. These different cases will be noted with an indice c varying from 1 to 3 for the contact conditions (1 is the full-contact condition, 2 and 3 are the one-point contact condition respectively on the left edge and on the right edge) and an indice i varying from 1 to 2 (1 is the impact on the left edge, 2 is the impact on the right edge). If we consider one of these contact conditions alone, then the model is no more hybrid and the number of degrees of freedom can be reduced to two: θ and l which is the same as for the classical inverse pendulum model. A state machine has been created in order to modify these contact conditions when the cart-table move. The model for the full and one-point contact is classically written [9]:

$$\begin{cases} \mathbf{M}(\mathbf{q})\ddot{\mathbf{q}} + \mathbf{N}(\mathbf{q}, \dot{\mathbf{q}})\dot{\mathbf{q}} + \mathbf{g}(\mathbf{q}) = \mathbf{J}_c^T(\mathbf{q})\boldsymbol{\lambda} + \mathbf{s}u \\ \mathbf{J}_c(\mathbf{q})\ddot{\mathbf{q}} + \boldsymbol{\Pi}_c(\mathbf{q}, \dot{\mathbf{q}}) = \mathbf{0} \end{cases} \quad (1)$$

$\mathbf{q} = [x, y, \theta, l]^T$ is the vector of generalized coordinates, $\mathbf{M}$ is the inertia matrix, $\mathbf{N}$ is the Coriolis and centrifugal matrix, $\mathbf{g}$ is the potential energy vector, $\boldsymbol{\lambda}$ is the vector of the forces of the contact points, $\mathbf{s}u$ is the command vector, $\mathbf{J}_c$ and $\boldsymbol{\Pi}_c$ are respectively the jacobian and the hessian of the equations of contact when the cart-table is in the contact situation c. The evolution of $\mathbf{q}$ is calculated by integrating this equation.

Newton's model is used as the impact model. It describes the transmission of the energy during the impact with a coefficient of restitution $\mathbf{E_v}$. Some more complex impact law can be studied like Moreau's law [10]. Additionally to this law, the integration of equation (1) over an infinitesimal

time interval when considering acceleration and forces as impulsional gives the system of equations:

$$\begin{cases} \mathbf{M}(\mathbf{q})(\dot{\mathbf{q}}_+ - \dot{\mathbf{q}}_-) = \mathbf{J}_i^T(\mathbf{q})\boldsymbol{\lambda}_i \\ \mathbf{J}_i(\mathbf{q})\dot{\mathbf{q}}_+ = -\mathbf{E_v}\mathbf{J}_i(\mathbf{q})\dot{\mathbf{q}}_- \end{cases} \quad (2)$$

$\dot{\mathbf{q}}_-$ and $\dot{\mathbf{q}}_+$ are respectively the speed of the generalized coordinates before and after the impact, $\boldsymbol{\lambda}_i$ is the vector of the integrated impulsional forces, $\mathbf{J}_i$ is the jacobian of the equations of contact during the impact i, $\mathbf{E_v}$ is the matrix of restitution from Newton's model. Thanks to this equation it is possible to obtain directly the speed of the generalized coordinates after impact from those before impact. Indeed equation (2) is equivalent to equation (3):

$$\begin{cases} \boldsymbol{\lambda}_i = -(\mathbf{J}_i\mathbf{M}^{-1}\mathbf{J}_i^T)^{-1}(\mathbf{I}_k + \mathbf{E_v})\mathbf{J}_i\dot{\mathbf{q}}_- \\ \dot{\mathbf{q}}_+ = \underbrace{(\mathbf{I}_4 - \mathbf{M}^{-1}\mathbf{J}_i^T(\mathbf{J}_i\mathbf{M}^{-1}\mathbf{J}_i^T)^{-1}(\mathbf{I}_i + \mathbf{E_v})\mathbf{J}_i)}_{\mathbf{E_q}(\mathbf{q})}\dot{\mathbf{q}}_- \end{cases}$$
$$(3)$$

$\mathbf{I}_n$ is the unit matrix of size n, 4 is the number of generalized coordinates and k is the number of contact constraints considered in the impact case i. The modified matrix of restitution $\mathbf{E_q}$ is the direct link between $\dot{\mathbf{q}}_+$ and $\dot{\mathbf{q}}_-$.

B. Implementing the model

The matrix $\mathbf{M}$, $\mathbf{N}$ and the vector $\mathbf{g}$ are classically calculated but we observe a particular property for the matrix $\mathbf{J}_i$ and thus the matrix $\mathbf{E_q}$. The jacobian of the constraints during the impact is:

$$\mathbf{J}_i(\mathbf{q}) = \begin{bmatrix} 0 & 1 & h_{G1}sin\theta - P_{max}cos\theta & 0 \\ 1 & 0 & h_{G1}cos\theta + P_{max}sin\theta & 0 \end{bmatrix} \quad (4)$$

From this observation, we can deduce that the speed of the cart before impact $\dot{l}_-$ has no effect on the angular speed after impact $\dot{\theta}_+$. It can also be observed with the matrix $\mathbf{E_q}$ whose last column is $[0, 0, 0, 1]^T$. Moreover, at the impact $\theta = 0$, so $\mathbf{E_q}$ is a function of l only: $\mathbf{E_q}(\mathbf{q}) = \mathbf{E_q}(l)$.

This hybrid model works around a state machine that can be partially seen in figure 4. This state machine indicates which model should be applied to calculate the dynamics, depending on the values of the state variables. In our case the successive states are 3 - 8 - 6 - 9 - 3. Since the phase 6 - 9 - 3 is symmetric with the phase 3 - 8 - 6, we will only work with half the cycle. The state machine jumps from 3 to 8 when $\theta = 0$ and from 8 to 6 when $\dot{\theta} < 0$. The system will be controlled during state 3 to reach state 8 with a precise speed. Then the system will evolve with free dynamics during phase 6.

C. Calculating the impact speed

The free dynamics of phase 6 is entirely determined by the dynamic equation (1) and the values of the state variable just after the impact $\boldsymbol{\zeta}_+ = [\theta_+, \dot{\theta}_+, l_+, \dot{l}_+]$. So the desired final position and speed at the end of the free dynamics $\boldsymbol{\zeta}_{df} = [\theta_{df}, \dot{\theta}_{df}, l_{df}, \dot{l}_{df}]$ is obtained by choosing the corresponding $\boldsymbol{\zeta}_+$. Finally, considering the matrix $\mathbf{E_q}$ and the impact at $\theta = 0$, it is possible to linked directly $\boldsymbol{\zeta}_{df}$ to the values of
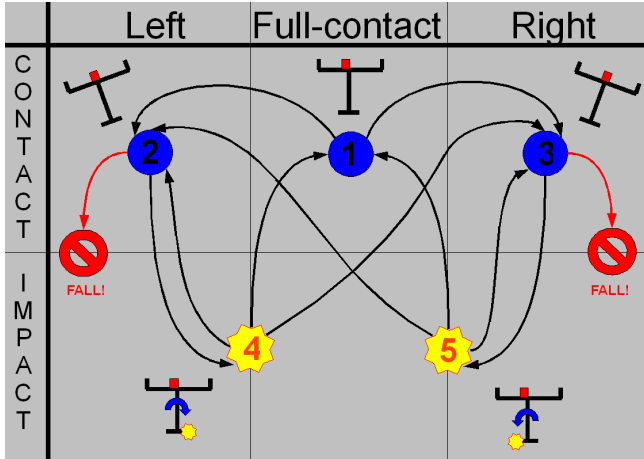
Fig. 4. The state machine of the cart-table

-

State 1: Full-contact state
State 2: Left-contact state
State 3: Right-contact state
State 4: Impact of the right edge of the table
State 5: Impact of the left edge of the table
State 6: Fall

Fig. 5. Classic and reverse dynamic of a falling ball

-

Objective: To determine the initial conditions $\mathbf{v}_0$ and z_0 that leads the classic dynamic to the final condition $\mathbf{v}_f$ and z_f
Method: Using the reverse dynamic (like watching a movie backward) with the initial conditions $-\mathbf{v}_f$ and z_f leads to the final condition $-\mathbf{v}_0$ and z_0

the state variable before the impact $\boldsymbol{\zeta}_-$. The key is to find a method to determine the initial condition of a system from its final condition and its dynamic equation.

This method consists in the reverse dynamics: it allows to calculate the dynamic of a system, starting from the end and thus to determine the initial condition. This method is very similar to a movie running backward and is illustrated with figure 5. If you choose the same image from a movie running backward and forward, the position of the objects will be the same in the two images but their velocity will be opposite. Thus, by integrating the dynamic equation (1) starting from the end with the values $[\theta_{df}, -\dot{\theta}_{df}, l_{df}, -\dot{l}_{df}]$, we obtain the values after impact $[\theta_+, -\dot{\theta}_+, l_+, -\dot{l}_+]$.

Here is a very simple demonstration for this method. If we consider the impact at $t = 0$ to simplify the equations, the classical integration of the dynamics gives:

$$\begin{cases} \boldsymbol{\zeta}_f - \boldsymbol{\zeta}_+ = \iint_0^{t_f} \ddot{\boldsymbol{\zeta}}(t)dt^2 \\ \dot{\boldsymbol{\zeta}}_f - \dot{\boldsymbol{\zeta}}_+ = \int_0^{t_f} \ddot{\boldsymbol{\zeta}}(t)dt \end{cases}$$

with the initial condition $\boldsymbol{\zeta}_+$. By replacing the variable $t' = t_f - t$ (backward variable), it gives:

$$\begin{cases} \boldsymbol{\zeta}_+ - \boldsymbol{\zeta}_f = \iint_0^{t_f} \ddot{\boldsymbol{\zeta}}(t_f - t')dt'^2 \\ -\dot{\boldsymbol{\zeta}}_+ - (-\dot{\boldsymbol{\zeta}}_f) = \int_0^{t_f} \ddot{\boldsymbol{\zeta}}(t_f - t')dt' \end{cases} \quad (5)$$

The system (5) shows that the reverse dynamics is obtained by interchanging initial and final position (from the first equation) and by interchanging initial and final velocity and taking their opposite (from the second equation). So it is really easy to obtain the values of the state variables after impact starting from the values at the end of the free dynamics thanks to the reverse dynamic. The values before
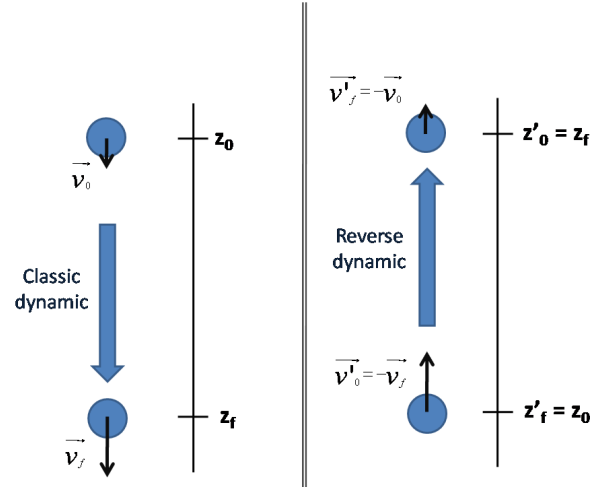
impact can then be determined by reversing the impact model as well. In our case it means the computation of the inverse of $\mathbf{E_q}$ since $\dot{q}_- = \mathbf{E_q^{-1}} \dot{q}_+$ gives the values of the state variables before impact. A control law has now to be designed to impact the ground with these precise values.

IV. PARTIAL LINEARIZATION BY STATE FEEDBACK

The robot is underactuated so all the state variables can't be exactly controlled. As a first step to test the global approach, a trajectory tracking on the variable θ has been selected. The trajectory was chosen in order to respect the desired value at the impact when no disturbance is applied. Then a nonlinear state feedback has been implemented to ensure a partial linearization of the equation (1) relatively to the variable θ. The characteristics of the trajectory tracking is tuned with two coefficients operating in the state feedback.

A. Linearizing the dynamic equation

According to the notations given in figure 3 the nonlinear model is:

$$\begin{cases} m_{11}\ddot{\theta} - M_2 h_{G2}\ddot{l} + 2M_2(P_{max} + l)\dot{\theta}\dot{l} + g_1 = 0 \\ -M_2 h_{G2}\ddot{\theta} + M_2\ddot{l} - M_2(P_{max} + l)\dot{\theta}^2 + M_2 g \sin\theta = u \end{cases}$$
$$(6)$$

m_{11} is the first-column first-row term of the inertia matrix $\mathbf{M}$ and g_1 is the first term of the potential energy vector $\mathbf{g}$:

$$\begin{cases} m_{11} &= I_T + M_1(P_{max}^2 + h_{G1}^2) \\ &\quad + M_2((P_{max} + l)^2 + h_{G2}^2) \\ g_1 &= g(M_1(P_{max}\cos\theta - h_{G1}\sin\theta) \\ &\quad + M_2((P_{max} + l)\cos\theta - h_{G2}\sin\theta) \end{cases}$$

	$Tr_{5\%} = 0.25s$		$Tr_{5\%} = 0.1s$	
$m = 0.1$	K_p =	400	K_p =	2500
	K_v =	4	K_v =	10
$m = 1$	K_p =	400	K_p =	2500
	K_v =	40	K_v =	100

TABLE II

VALUES OF THE COEFFICIENTS K_p AND K_v DEPENDING ON THE
VALUES OF THE 5% RESPONSE TIME FOR A $1s$ SIMULATION AND THE
DAMPING RATIO m

In order to linearize this system relatively to the variable θ, we must choose u such that:

$$u = 2M_2 \frac{P_{max}+l}{h_{G2}} \dot{\theta}\dot{l} - M_2(P_{max}+l)\dot{\theta}^2 + \frac{g_1}{h_{G2}} + M_2 g \sin\theta$$
$$+ \frac{m_{11} - m_2 h_{G2}^2}{h_{G2}} (\ddot{\theta}_d + K_v(\dot{\theta}_d - \dot{\theta}) + K_p(\theta_d - \theta)) \quad (7)$$

K_p and K_v are coefficients whose tuning will give the characteristics of the trajectory tracking (damping and speed).

The linearized system is then:

$$\begin{cases} \ddot{\theta} = \ddot{\theta}_d + K_v(\dot{\theta}_d - \dot{\theta}) + K_p(\theta_d - \theta) \\ \ddot{l} = \frac{u}{M_2} + h_{G2}\ddot{\theta} + (P_{max}+l)\dot{\theta}^2 - g\sin\theta \end{cases} \quad (8)$$

Two choices are necessary to determine completely u. The first one is the reference trajectories $\ddot{\theta}_d$, $\dot{\theta}_d$ and θ_d and the second one is the coefficient K_p and K_v in order to tune the reactivity of the trajectory tracking after a disturbance.

B. Calculating the reference trajectory

A 6 degrees polynomial has been chosen to define the reference trajectory for θ. Two others are determined by the initial conditions $[\theta_0, \dot{\theta}_0]$ and two other degrees by the desired conditions before impact $[\theta_{-d}, \dot{\theta}_{-d}]$. Lastly $[\mu_1 = \ddot{\theta}_0, \mu_2 = \ddot{\theta}_-]$ are used as parameters of an optimization problem. This problem forces the values before impact $[l_-, \dot{l}_-]$ to be the closest possible to the desired values $[l_{-d}, \dot{l}_{-d}]$:

$$\begin{cases} \min_{\mu_1,\mu_2} J = k_1(l_- - l_{-d})^2 + k_2(\dot{l}_- - \dot{l}_{-d})^2 + k_3 u^2 \\ \theta_d = P(\mu_1, \mu_2) \\ (6) \text{and} \zeta_0 \\ (7) \end{cases} \quad (9)$$

$\zeta_0 = [\theta_+, \dot{\theta}_+, l_+, \dot{l}_+]$ are the initial conditions to be used with the dynamic equation (6), k_1 and k_2 are coefficient which weight the state, enabling to give a greater importance to the position or the velocity of l before impact when no exact solution exists. k_3 when different from 0 adds the minimization of the command energy to the optimization problem. With the solution (μ_1, μ_2) the reference trajectory is completely defined. Thus we obtain the desired trajectory θ_d and by derivation $\dot{\theta}_d$ and $\ddot{\theta}_d$.

C. Choosing the coefficients to track the trajectory

The values of K_p and K_v rule the behavior of the system with regard to the disturbances by reducing the error
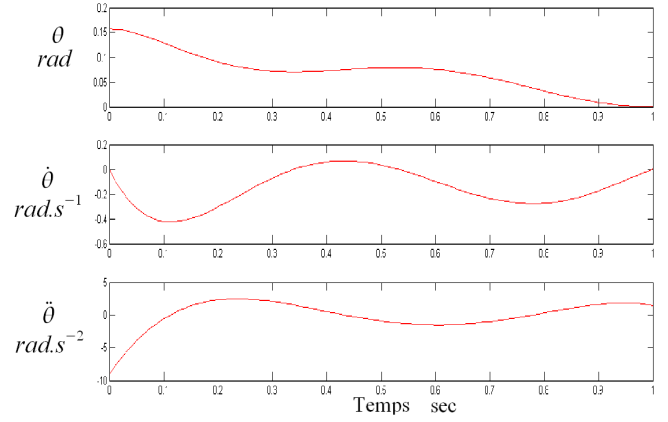

Fig. 6. Reference trajectories to ensure stop at the end of the step. The duration has been arbitrarily fixed to 1s.

between the desired value of θ and its real value. With these two coefficients it is possible to tune the response time ($Tr_{5\%}$ is the time response so that the error between the real and the desired value is less than 5% of the real value) and the oscillations (m is the damping ratio which indicates the amplitude of the oscillations). Some values of the coefficients K_p and K_v along with the characteristics associated are presented in table II. Those results has been calculated from the expression of K_p and K_v:

$$\begin{cases} K_v = 2m\omega_0 \\ K_p = \omega_0^2 \end{cases}$$

ω_0 is the natural pulsation obtained from the damping ratio m, the 5% response time $Tr_{5\%}$ and the classical time response graph.

V. TWO CONCRETE EXAMPLES AND SIMULATIONS

In order to illustrate this method, here are two concrete examples. The first one explains how to stop the cart-table by zeroing the speed of the state variables at the impact with the ground. From this example we will extract the values of K_p and K_v adapted to our system. The second example deals with the realization of a full step and every details of the method are explained.

A. Example 1: Stopping the walking with minimization of the command energy

In this example the goal is to stop the cart. According to our method, the impact speed of the state variables must then be zeroed: $\dot{\theta}_- = 0$ and $\dot{l}_- = 0$. Thus, from equation (2), the robot will stop whatever the matrix restitution $\mathbf{E_q}$ is. Moreover, we must add the static balance equation to ensure that the robot does not move after the impact. It means that the projection of the CoM on the ground must lie inside the support polygon. The best way of enforcing this criterion is to force l to be as close as possible from 0 at the end of the step. This part is implemented in the expression of

Fig. 7. Reference trajectories (dotted line) and real trajectory (plain line) of the four state variables with $K_p = 400$ and $K_v = 40$
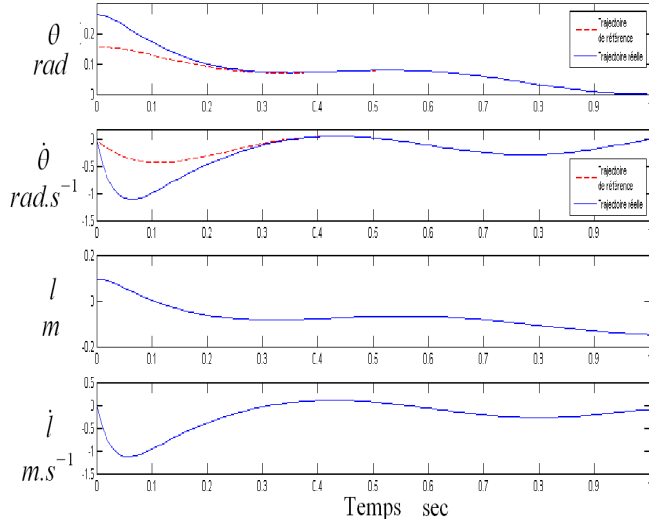

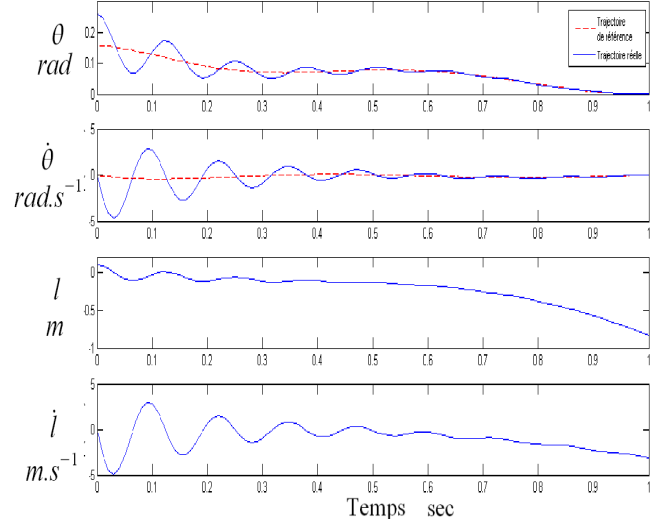Fig. 8. Reference trajectories (dotted line) and real trajectory (plain line) of the four state variables with $K_p = 2500$ and $K_v = 10$

the cost of the optimization problem along with a term of minimization of the command energy:

$$\begin{cases} \min_{\mu_1, \mu_2} J = k_1 l_-^2 + k_2 \dot{l}_-^2 + k_3 \mathbf{u}^T \mathbf{u} \\ \theta_d = P(\mu_1, \mu_2) \\ (6) \oplus \boldsymbol{\zeta}_0 \\ (7) \end{cases} \quad (10)$$

In this case, we choose $k_2 \gg k_1, k_3$ so that the main condition $\dot{l}_- = 0$ weights bigger than the secondary condition. By choosing $k_1, k_3 = 1$ and $k_2 = 10^5$, with the initial conditions $\theta_0 = \frac{\pi}{20}$ and $\dot{\theta}_0 = 0$, the reference trajectories θ_d, $\dot{\theta}_d$ and $\ddot{\theta}_d$ are shown in figure 6.

With these reference trajectories $\dot{\theta}$ is exactly zeroed when $\theta_- = 0$. It is also possible to read the results of the optimization problem on the last curve of figure 6:

$$\begin{cases} \mu_1 \simeq -9s^{-2} \\ \mu_2 \simeq 1.5s^{-2} \end{cases}$$

In order to study the trajectory tracking, a significant disturbance has been introduced at the beginning of the simulation. Indeed the initial condition on θ have been set to $\theta_0 = \frac{\pi}{12}$ whereas the value used to generate the trajectory was $\theta_0 = \frac{\pi}{20}$. The results of this simulation are presented in figure 7 and 8 with different values for K_p and K_v.

These curves give two important leads to choose the coefficient K_p and K_v. Regarding the two first curves of each graph concerning θ and $\dot{\theta}$, we observe some considerable oscillations when $m = 0.1$. This behavior may cause undesired impact between the table and the ground. So selecting K_p and K_v such that $m = 0.1$ avoid this issue. Furthermore regarding the two last curves of each graph concerning l and $\dot{l}$, we do not obtain exactly the values before impact which was stated by the optimization problem. Indeed the system is underactuated and the tracking is done to fit the trajectory of θ. Thus any disturbance on θ induces significant variations on u and so on l. That is why a
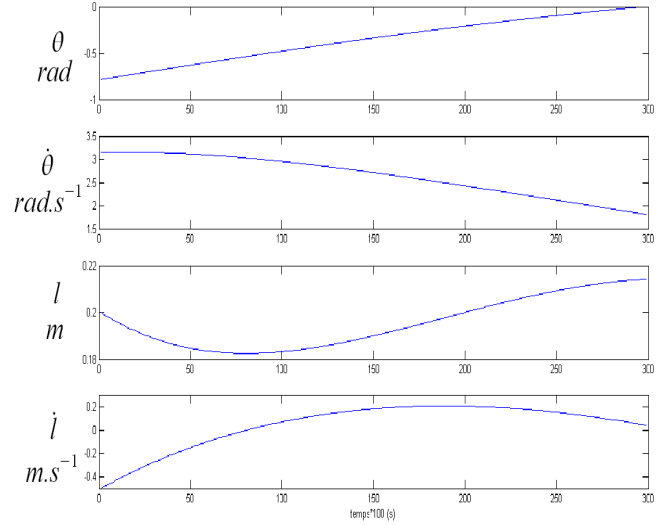

Fig. 9. Results of the reverse dynamic on the four state variables

fast non-oscillatory behavior leads to values of l and $\dot{l}$ closer to the ones desired. In our simulation we then choose $K_p = 400$ and $K_v = 40$ which leads to such a behavior.

B. Example 2: Generation of a full step

In this example, the complete methodology to generate a full step is exposed. Firstly we must decide the values of the state variables we wish to reach at the end of the free dynamic phase. Let's choose:

$$\begin{cases} \theta_f &= -\frac{\pi}{4} \\ \dot{\theta}_f &= -\pi s^{-1} \\ l_f &= 0.2m \\ \dot{l}_f &= 0.5m.s^{-1} \end{cases}$$

Secondly, using the reverse dynamic method and feeding it with the initial conditions $\theta_{ini} = \theta_f$, $\dot{\theta}_{ini} = -\dot{\theta}_f$, $l_{ini} =$

	As a function of $\dot{\theta}_+$ and $\dot{l}_+$	In our example
inelastic impact $(e = 1)$	$\begin{cases} \dot{\theta}_+ = \dot{\theta}_- \\ \dot{l}_+ = \dot{l}_- \end{cases}$	$\begin{cases} \dot{\theta}_- = 1.8s^{-1} \\ \dot{l}_- = 0m.s^{-1} \end{cases}$
intermediary impact $(e = 0.5)$	$\begin{cases} \dot{\theta}_+ = \dfrac{\dot{\theta}_-}{2} \\ \dot{l}_+ = \dot{l}_- - 0.45\dot{\theta}_- \end{cases}$	$\begin{cases} \dot{\theta}_- = 3.6s^{-1} \\ \dot{l}_- = 1.62m.s^{-1} \end{cases}$
elastic impact $(e = 0)$	$\begin{cases} \dot{\theta}_+ = 0 \\ \dot{l}_+ = \dot{l}_- - 0.9\dot{\theta}_- \end{cases}$	No solution

TABLE III

RELATIONSHIP BETWEEN SPEED BEFORE AND AFTER IMPACT AS A FUNCTION OF e AND EFFECTIVE VALUES FOR OUR EXAMPLE
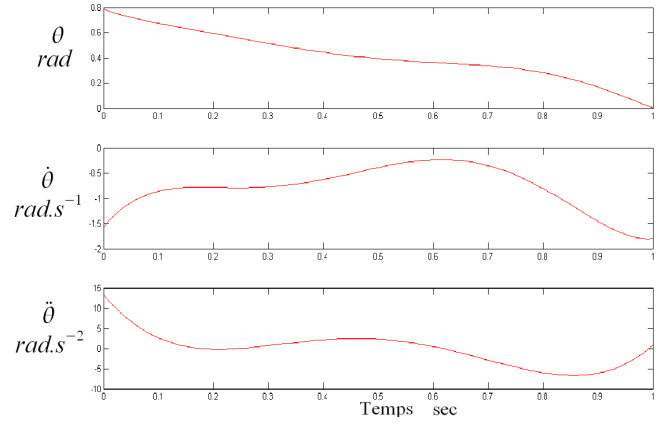

Fig. 10. Reference trajectories to ensure an impact with $\dot{\theta}_- \simeq 1.8s^{-1}$, $l_- \simeq 0.22m$ and $\dot{l}_- \simeq 0m.s^{-1}$. The duration has been arbitrarily fixed to 1s.

l_f and $\dot{l}_{ini} = \dot{l}_f$, we can determined the values of the state variables just after the impact. These values are read at the end of the simulation shown in figure 9 (the simulation ends when $\theta = 0$):

$$\begin{cases} \theta_+ = 0 \\ \dot{\theta}_+ \simeq 1.8s^{-1} \\ l_+ \simeq 0.22m \\ \dot{l}_+ \simeq 0m.s^{-1} \end{cases}$$

Thirdly equation (3) enables the calculation of the values of the state variables just before the impact depending on the restitution matrix $\mathbf{E}_v$. If we consider this matrix of the form:

$$\mathbf{E}_v = \begin{bmatrix} 0 & e \\ e & 0 \end{bmatrix}$$

with e the restitution coefficient, table III sums up the effect of the choice of this coefficient on the values of the state variables before impact. This table shows that this method does not work if we consider a dissipative impact ($e = 0$). If so no energy can be restituted to the free dynamic and the robot cannot move further. For this example we thus consider the impact as completely inelastic and we deduce the values of the state variable just before impact:

$$\begin{cases} \theta_- = 0 \\ \dot{\theta}_- \simeq 1.8s^{-1} \\ l_- \simeq 0.22m \\ \dot{l}_- \simeq 0m.s^{-1} \end{cases}$$

Lastly we must generate the control law that lead our robot to this pre-impact state. The reference trajectory is defined by the solution of the optimization problem:

$$\begin{cases} \min_{\mu_1, \mu_2} J = k_1(l_- - 0.22)^2 + k_2\dot{l}_-^2 \\ \theta_d = P(\mu_1, \mu_2) \\ (6) \text{and} \boldsymbol{\zeta}_0 \\ (7) \end{cases}$$

As velocity has no reason to be more important than the position in this case, we choose $k_1 = k_2 = 1$. The reference trajectory obtained are shown in figure 10.

The full step is completely defined. The system must now calculate u at each time step from the values of the current state variables using equation (7).

Fig. 11. The mechanical prototype of the cart-table

VI. CONCLUSION AND FUTURE WORKS

This paper proposes a new method to implement a control law for biped robot based on a two-phase step and control of the velocity when the foot of the robot impact the ground. This method is presented on a simplified model: the cart-table. It can be summed up in this way:

- Decomposing the step in two phase: the free dynamic phase and the impact preparation phase.
- Choosing values at the end of the free dynamic for the state variables.
- Determining the corresponding values of the state variables just after the impact by using the reverse dynamic method.
- Determining the corresponding values of the state variables just before the impact by using the restitution matrix.
- Calculating an optimal reference trajectory that enables to reach the desired pre-impact values of the state variables.
- Calculating the command at each time step from the error between the reference and the real trajectory.

Even though this rough method brings interesting results, many improvements could refine it.

Our future works will concentrate on different tracks. The priority one is to design a control law for the impact prepa-

ration phase that is much consistent with an underactuated system like the cart-table. Then we will try the full method on the cart-table prototype shown in figure 11. Afterwards more subtle improvements could be made, especially about the impact model.

The final goal is to transcribe this method on the prototype SHERPA in consideration of its desired walking speed. Moreover this speed must be adaptive to the speed of the person leading SHERPA. Thus an important work on the definition of the value of the state variables at the end of the free dynamic should be done along with the definition of the step length.

REFERENCES

[1] M. VUKOBRATOVIC and B. BOROVAC, "Zero-moment point - thirty five years of its life," *International Journal of Humanoid Robotics*, vol. 1, no. 1, pp. 157–173, 2004.

[2] S. KAJITA, F. KANEHIRO, K. KANEKO, K. FUJIWARA, K. HARADA, K. YOKOI, and H. HIRUKAWA, "Biped walking pattern generation by using preview control of zero-moment point," in *International Conference on Robotics and Automation*, sep.

[3] *ASIMO Technical Information*.

[4] A. GOSWAMI, "Postural stability of biped robots and the foot rotation indicator (fri) point," *International Journal of Robotics Research*, jul.

[5] J. W. GRIZZLE, C. CHEVALLEREAU, and C.-L. SHIH, "Asymptotically stable walking of a simple underactuated 3d bipedal robot," in *Industrial Electronics Conference*, nov.

[6] P. MANOONPONG, T. GENG, B. PORR, and F. WORGOTTER, "The runbot architecture for adaptative, fast, dynamic walking," in *IEEE International Symposium on Circuits and Systems*, may 2007.

[7] J. PRATT, C.-M. CHEW, A. TORRES, P. DILWORTH, and G. PRATT, "Virtual model control: An intuitive approach for bipedal locomotion," *International Journal of Robotics Research*, vol. 20, no. 2, pp. 129–143, 2001.

[8] P. GARREC, J.-P. FRICONNEAU, and F. LOUVEAU, "Virtuose 6d: A new force-control master arm using innovative ball-screw actuators," in *International Symposium on Robotics*, 2004.

[9] M. W. SPONG and M. VIDYASAGAR, *Robot Dynamics and Control*. John Wiley, 1989.

[10] B. BROGLIATO, Ed., *Impacts in Mechanical Systems. Analysis and Modeling*. Springer Verlag, 2000.